Title

Amyloid β Ion Channels in a Membrane Comprising Brain Total Lipid Extracts

Journal

ACS Chemical Neuroscience, 8(6)

ISSN

1948-7193

Authors

Lee, Joon

Kim, Young Hun

Arce, Fernando T

et al.

Publication Date

2017-06-21

DOI

10.1021/acschemneuro.7b00006

Peer reviewed

ACS Chemical Neuroscience

Research Article

pubs.acs.org/chemneuro

Amyloid β Ion Channels in a Membrane Comprising Brain Total Lipid Extracts

Joon Lee,[†] Young Hun Kim,[†] Fernando T. Arce,[‖] Alan L. Gillman,[§] Hyunbum Jang,[⊥] Bruce L. Kagan,[#] Ruth Nussinov,[⊥] Jerry Yang,[†,‡] and Ratnesh Lal*[,†,§,△]

[†]Materials Science and Engineering, [‡]Department of Chemistry and Biochemistry, [§]Department of Bioengineering, and [△]Department of Mechanical and Aerospace Engineering, University of California—San Diego, La Jolla, California 92093, United States

[‖]Division of Translational and Regenerative Medicine, Department of Medicine, Department of Biomedical Engineering, University of Arizona, Tucson, Arizona 85721, United States

[⊥]Cancer and Inflammation Program, National Cancer Institute at Frederick, Leidos Biomedical Research, Inc., Frederick National Laboratory for Cancer Research, Frederick, Maryland 21702, United States

[#]Department of Psychiatry, David Geffen School of Medicine, Semel Institute for Neuroscience and Human Behavior, University of California, Los Angeles, California 90024, United States

Supporting Information

ABSTRACT: Amyloid β (Aβ) oligomers are the predominant toxic species in the pathology of Alzheimer's disease. The prevailing mechanism for toxicity by Aβ oligomers includes ionic homeostasis destabilization in neuronal cells by forming ion channels. These channel structures have been previously studied in model lipid bilayers. In order to gain further insight into the interaction of Aβ oligomers with natural membrane compositions, we have examined the structures and conductivities of Aβ oligomers in a membrane composed of brain total lipid extract (BTLE). We utilized two complementary techniques: atomic force microscopy (AFM) and black lipid membrane (BLM) electrical recording. Our results indicate that $Aβ_{1-42}$ forms ion channel structures in BTLE membranes, accompanied by a heterogeneous population of ionic current fluctuations. Notably, the observed current events generated by $Aβ_{1-42}$ peptides in BTLE membranes possess different characteristics compared to current events generated by the presence of $Aβ_{1-42}$ in model membranes comprising a 1:1 mixture of DOPS and POPE lipids. Oligomers of the truncated Aβ fragment $Aβ_{17-42}$ (p3) exhibited similar ion conductivity behavior as $Aβ_{1-42}$ in BTLE membranes. However, the observed macroscopic ion flux across the BTLE membranes induced by $Aβ_{1-42}$ pores was larger than for p3 pores. Our analysis of structure and conductance of oligomeric Aβ pores in a natural lipid membrane closely mimics the in vivo cellular environment suggesting that Aβ pores could potentially accelerate the loss of ionic homeostasis and cellular abnormalities. Hence, these pore structures may serve as a target for drug development and therapeutic strategies for AD treatment.

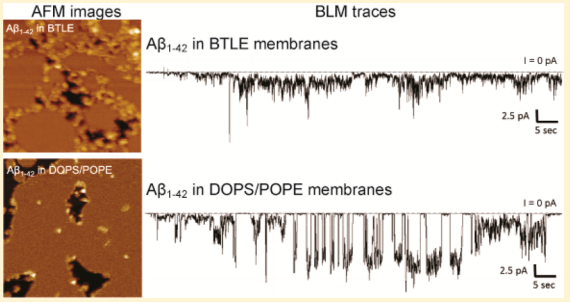

KEYWORDS: *Alzheimer's disease, amyloid β peptides, amyloid channels, brain total lipid extract, amyloid−membrane interactions, atomic force microscopy, black lipid membrane electrophysiology*

INTRODUCTION

Alzheimer's disease (AD) is one of the most devastating neurodegenerative diseases. It is characterized by the progressive loss of memory and cognition. One of the pathological hallmarks of AD is the deposition of fibrillar amyloid plaques in the brains of AD patients.[1] Amyloid beta (Aβ) peptides, the major constituents of these plaques, are derived by enzymatic cleavage from the transmembrane amyloid precursor protein (APP); a process involving α-, β-, and γ-secretases. The full length $Aβ_{1-40/42}$ is produced by cleavage of APP by β- and γ-secretases, and the smaller hydrophobic $Aβ_{17-42}$ (p3) fragment is produced by α- and γ-secretase APP cleavage.[2−5]

Although accumulation of Aβ plaques in AD brains was believed to be directly correlated to the disease, increasing evidence indicates that small Aβ oligomers are the main toxic species.[6,7] However, the exact disease mechanism has not yet been fully elucidated. A prevailing mechanism of AD pathology postulates that Aβ oligomers negatively affect neuronal function and survival by forming ion permeable pores, resulting in the destabilization of cell ionic homeostasis.[8−12] This hypothesis is supported by data from several experimental techniques and molecular dynamics (MD) simulations studying Aβ-induced

Received: January 6, 2017
Accepted: January 30, 2017
Published: January 30, 2017

DOI: 10.1021/acschemneuro.7b00006
ACS Chem. Neurosci. 2017, 8, 1348−1357

permeability of ions across model lipid membranes,[9,10,13,14] as well as an "optical patch clamp" method whereby total internal reflection fluorescence (TIRF) microscopy data revealed the presence of localized Ca^{2+} transients during cellular influx across *Xenopus* oocyte membranes.[15]

The p3 fragment represents an additional source of toxicity from APP processing that contributes to neuronal cell death.[4,16] It was shown that $A\beta_{22-35}$ peptides induce specific increases of Ca^{2+} levels in neural cells; these effects of $A\beta$ oligomers on cellular Ca^{2+} influx could be inhibited by zinc ions.[17] We have previously shown that the p3 and $A\beta_{9-42}$ (N9) fragments form pores in black lipid membranes (BLM) and permeabilize the membranes of neuronal cells.[4,18]

The structure and function of these Ca^{2+}-flux inducing $A\beta$ pores have been primarily studied using in vitro techniques. Atomic force microscopy (AFM) and electron microscopy (EM) have been the most frequently utilized imaging techniques for examining the structure of $A\beta$ pores in model membranes because of their high-resolution capabilities.[9,19,20] AFM images of $A\beta$ oligomers reconstituted in model lipid bilayers show porelike structures with outer pore diameters of 8−12 nm.[21−23] Electrical recording data obtained for various $A\beta$ oligomers in planar lipid membranes display the heterogeneous multiple conductances characteristic of $A\beta$ and all amyloid peptides studied to date.[14,24] These current fluctuations show weak cation selectivity, voltage independence, inhibition by Congo red, and reversible blockage by Zn^{2+} ions.[10,25,26] Previously, we compared the pore activities and structures of $A\beta_{1-42}$ and $A\beta_{pE3-42}$ in anionic lipid membrane comprised of DOPS/POPE (1:1, wt/wt).[23,24] Because of the post translational cleavage of amino acid residues 1 (Asp) and 2 (Ala) (of which amino acid 1 is a negatively charged residue at neutral pH) and modification of the 3 (Glu) residue to the hydrophobic pyroglutamate (pE), $A\beta_{pE3-42}$ oligomeric subunits are more hydrophobic and more stable in the membrane allowing larger transient pore structures to form than for $A\beta_{1-42}$ pores, resulting in larger ion conductance of $A\beta_{pE3-42}$ pores.[24]

Most of these previous studies were conducted in model lipid membranes, not thoroughly displaying all of the structural complexities of a mixture of lipids found in natural cellular membranes. Cell membranes contain various lipids that work cooperatively in specialized domains.[27] AD brains have been shown to contain and increased fraction of anionic lipids such as phosphatidylserine (PS) and phosphatidylglycerol (PG) compared to the brains of cognitively normal patients, while the percentage of neutral lipids like phosphatidylcholine (PC) remains simliar.[28] Also, anionic lipids, but not neutral lipids, show dose dependent increase in cation influx by $A\beta$ peptides[29] and the pore activity in anionic lipid membranes was decreased when cholesterol was introduced.[30,31] These findings suggest the possible role of negatively charged lipids in permeability induced by $A\beta$ peptides. Our prior work in this field has focused primarily on DOPS/POPE membranes as an extreme model of the anionic lipid membrane found in progressed AD patients. To better simulate the initial pathogenesis of AD, here we used a membrane comprised of natural brain total lipid extracts (BTLE) which is considered to be the closest mimic of the healthy (or very early AD stage) neuronal membrane.[32] In the present study, we study the structures and ion conducting of $A\beta$ peptides in BTLE membranes. We utilized two complementary techniques, AFM and BLM electrical recordings, to identify and characterize the biophysical properties of $A\beta_{1-42}$ pore formation and examined the structure and ion conducting properties of $A\beta$ pores in BTLE membranes and compared with the anionic DOPS/POPE (1:1, wt/wt) membranes. Our AFM images reveal porelike structures for the $A\beta_{1-42}$ peptides in both BTLE and DOPS/POPE membranes. Interestingly, the ion conducting activity of $A\beta_{1-42}$ in BTLE membranes exhibits notable differences when compared with the ion conducting properties of these peptides in DOPS/POPE membranes. We observed similar difference in the ion conducting behavior of p3 peptides when incorporated in BTLE vs DOPS/POPE membranes. These studies reveal that both full-length $A\beta$ and its nonamyloidogenic p3 fragment form pores in natural BTLE membranes, suggesting that both peptides have the capability to alter neuronal cell homeostasis and play toxic roles in AD.

RESULTS AND DISCUSSION

Interaction with BTLE or DOPS/POPE Liposomes Facilitates the Self-Assembly Behavior of $A\beta$. Thioflavin T (ThT) molecules are often used to monitor the self-assembly kinetics of $A\beta$, as ThT molecules show enhanced fluorescence intensity upon binding to β sheet structures in amyloid fibrils.[33,34] Here, we used ThT fluorescence to monitor the self-assembly kinetics of $A\beta_{1-42}$ in the presence of liposomes comprised of DOPS/POPE (1:1, wt/wt) or BTLE (Figure 1).

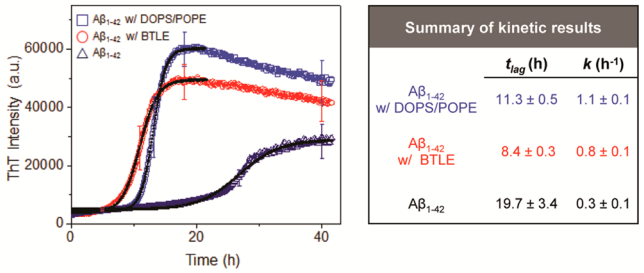

Figure 1. Self-assembly of $A\beta_{1-42}$ in the presence of BTLE and DOPS/POPE (1:1, wt/wt) liposomes monitored by ThT fluorescence. ThT fluorescence intensity of $A\beta_{1-42}$ in the presence of DOPS/POPE (blue square) or BTLE (red circle) increased faster than the ThT fluorescence intensity of $A\beta_{1-42}$ alone (dark blue triangle). t_{lag} and k were obtained by fitting the data from ThT fluorescence using eq 1 (given in the Methods section). The fitted curves are shown in black line. ThT fluorescence was measured every 5 min at 25 °C after stirring for 2 s. In these experiments, a 10 μM solution of $A\beta_{1-42}$ was incubated with or without BTLE or DOPS/POPE liposomes in 10 mM HEPES (150 mM KCl, 1 mM $MgCl_2$) buffer. Data represent an average from 5 independent measurements, and the standard deviation was used for error bar.

We examined the effect of anionic lipid (DOPS) which is one of the major known compositions of BTLE on $A\beta_{1-42}$ self-assembly although the structural identity of ∼60% of the lipids in BTLE samples is unknown (see Supporting Information Table 1). All ThT fluorescence traces show a sigmoidal trend indicating a growth of β sheet containing fibril structures.[35−37] At the initiation of each experiment, we observed low ThT intensity, indicating the absence of noticeable β-sheet structures. This low initial intensity remained approximately constant for the first few hours, and only a slight increase in ThT fluorescence was observed during this period. In this phase, known as the lag phase time (t_{lag}), monomers aggregate into small oligomers to form nucleates or seeds.[36,38] The ThT intensity then rapidly increased as small $A\beta$ oligomers

DOI: 10.1021/acschemneuro.7b00006
ACS Chem. Neurosci. 2017, 8, 1348−1357

elongated into fibrils and the fluorescence reached the final equilibrium phase. Notably, Aβ_{1-42} started self-assembly faster when either BTLE (red circle) or DOPS/POPE (blue square) liposomes were present in the solution compared to observed aggregation kinetics of Aβ_{1-42} in lipid-free solution (dark blue triangle). These results indicate that the presence of a membrane surface plays an important role in self-assembly of Aβ_{1-42}.

The observed time-course of ThT fluorescence curves were background corrected by subtracting the ThT fluorescence curve without Aβ_{1-42} for Aβ_{1-42} in lipid-free solution or ThT fluorescence curve with the liposomes (either BTLE or DOPS/POPE) in solution for Aβ_{1-42} with the liposomes, respectively and were fitted using eq 1.[23,36]

$$F = F_0 + \frac{a}{1 + e^{-k(t-t_{ht})}} \quad (1)$$

where t is time, t_{ht} is the time it takes to get half-maximal ThT fluorescence, F_0 is the initial ThT fluorescence intensity, a is the amplitude of the highest intensity, and k is the rate constant. The lag phase time (t_{lag}) was calculated from the fitting parameters obtained above using eq 2.

$$t_{lag} = t_{ht} - \frac{2}{k} \quad (2)$$

From the fitted curves (black solid lines) in Figure 1, we obtained a t_{lag} of 8.4 ± 0.3 h for Aβ_{1-42} with BTLE liposomes, 11.3 ± 0.5 h for Aβ_{1-42} with DOPS/POPE, and 19.7 ± 3.4 h for Aβ_{1-42} alone. The shortest observed t_{lag} for Aβ_{1-42} aggregation was in BTLE membranes suggesting that the mixture of various lipids present in BTLE might increase the speed of the formation of seeds. The low ThT fluorescence intensity at this initial phase of the aggregation process suggests that there are very few protofibril species in solution. Previous reports from AFM experiments reveal small globular shape of Aβ oligomers[23,39] and from structural NMR experiments of Aβ_{1-40} in this phase reveals a partially folded structure forming a 3_{10} helix[40] and the presence of oligomers containing α-helix and reversible β-sheet structures.[41]

Although the observed t_{lag} for Aβ_{1-42} was shortest in the presence of BTLE liposomes, the aggregation rate constant (k) of Aβ_{1-42} with DOPS/POPE (1.1 ± 0.1 h^{-1}) was faster than Aβ_{1-42} with BTLE (0.8 ± 0.1 h^{-1}) or Aβ_{1-42} alone (0.3 ± 0.1 h^{-1}). These results suggest that Aβ_{1-42} peptides prefer more to form seeds with BTLE than to elongate into fibrils compared to the seeds formed with DOPS/POPE. As small oligomeric Aβ species are found to play a more prominent role in AD neuropathology[42,43] than, e.g., Aβ fibrils, the structure of these oligomeric species in the lipid membranes and the electrophysiological activities were studied using AFM and BLM.

Distribution of Aβ_{1-42} Oligomer Structures on BTLE and DOPS/POPE Membranes. We employed AFM to study the porelike structures and surface interactions of Aβ_{1-42} oligomers in BTLE and DOPS/POPE (1:1, wt/wt) membranes. As a control, intact BTLE membranes that were not exposed to Aβ_{1-42} oligomers were imaged. The untreated membrane (bright region, Figure 2A) had a flat and smooth surface with a bilayer thickness of ~5.4 nm, in agreement with previous reports on the thickness of DOPS/POPE membrane (~5 nm).[23] When Aβ_{1-42} oligomers were reconstituted at 1:20 peptide to lipid mass ratio in a BTLE membrane, we observed a large population of small annular objects protruding 1−2 nm out of the plane of the membrane (Figure 2B). Structures

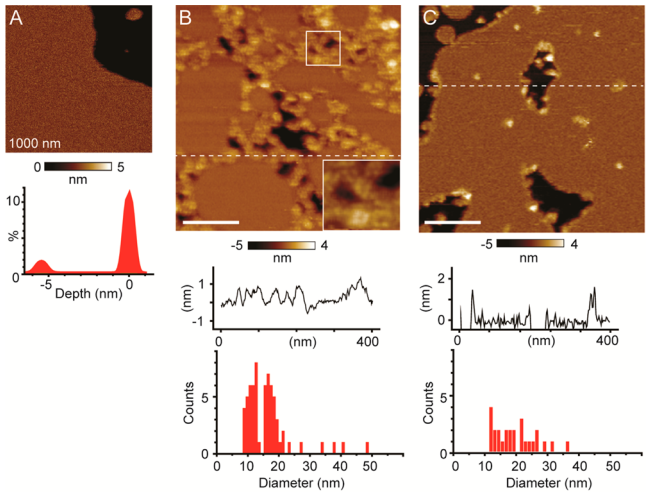

Figure 2. AFM images of reconstituted Aβ_{1-42} oligomers in BTLE or DOPS/POPE supported lipid membranes on mica. (A) AFM image of a BTLE membrane in the absence of Aβ. The dark region in right top corner is the mica surface. A depth histogram reveals a membrane thickness of 5.4 nm. (B) AFM image of a BTLE membrane reconstituted with Aβ_{1-42} oligomers (1:20 peptide/lipid mass ratio). Numerous small porelike structures are visible at higher magnification (inset: 50 × 50 nm^2 area). The cross section analysis from the dashed line shows most of the oligomers protrude <1 nm from the membrane surface. Histograms representing the frequency of Aβ_{1-42} oligomers as a function of diameter shown below the cross section analysis reveal populations of oligomers mostly ranging from 9−20 nm. (C) AFM image of a DOPS/POPE membrane with Aβ_{1-42} oligomers (1:20 peptide/lipid mass ratio). Only sparsely populated small Aβ_{1-42} oligomers were found. The cross section analysis from the dashed line in the AFM image shows the heights of small features protrude mostly ~1 nm from the membrane surface with some larger Aβ_{1-42} oligomers. Both the cross sectional height estimates and the histograms of the diameters of Aβ_{1-42} oligomers were generated using a Nanoscope Analysis program. Scale bars represent 100 nm.

containing features that protrude <1.5 nm protruding outside of the plane of the membrane were interpreted to be Aβ oligomers inserted in the membrane. Their surface density was estimated to be 300−500 oligomers/μm^2 and the majority of these structures had measured diameters between 10−20 nm (Figure 2B). Two predominant subpopulations of oligomers with diameters centered around 12 and 16.5 nm were observed. One of these subpopulations centered around 12 nm displayed porelike structures (inset, Figure 2B), comparable to those previously observed with Aβ oligomers inserted into synthetic lipids.[9,10,22,44] In addition, we observed another minor subpopulation of larger oligomers partitioned on the bilayer surface with heights of 3−4 nm above the membrane plane. In DOPS/POPE membranes, Aβ_{1-42} oligomers had heights ranging from 1−5 nm outside the membrane plane, and diameters ranging from 10−38 nm (Figure 2C). We found that the density of Aβ_{1-42} oligomers was lower in DOPS/POPE membranes compared to BTLE membranes, although more of larger oligomers were present in DOPS/POPE membranes. This result suggests that more oligomers interact with the surfaces of BTLE membranes than with membranes comprised of DOPS/POPE and might be responsible for the shorter t_{lag} of Aβ_{1-42} in BTLE liposomes.

Pore Structures of Aβ_{1-42} in BTLE and DOPS/POPE Membranes. Computational studies can provide predictions of membrane-bound conformations of the Aβ pores with

DOI: 10.1021/acschemneuro.7b00006
ACS Chem. Neurosci. 2017, 8, 1348−1357

atomic-level detail. Anionic DOPS/POPE (1:2 molar ratio) lipid membranes were used to simulate the pore structure of $A\beta_{1-42}$. We modeled $A\beta_{1-42}$ pores in a β-barrel topology using two $A\beta_{1-42}$ conformers with the β-strand-turn-β-strand motif in a similar manner as we reported in previous computational studies.[22,45,46] Explicit MD simulations on $A\beta_{1-42}$ barrels embedded in the DOPS/POPE membrane provided fully relaxed pore conformations in the lipid environment.[45] For the 18-mer barrels, the calculated averaged pore diameter and the maximum pore height across the bilayer are ~7.9 and ~6.9 nm for the conformer 1, and ~8.0 and ~6.8 nm for the conformer 2 barrels (Figure 3A). The lateral pore diameter depends on the

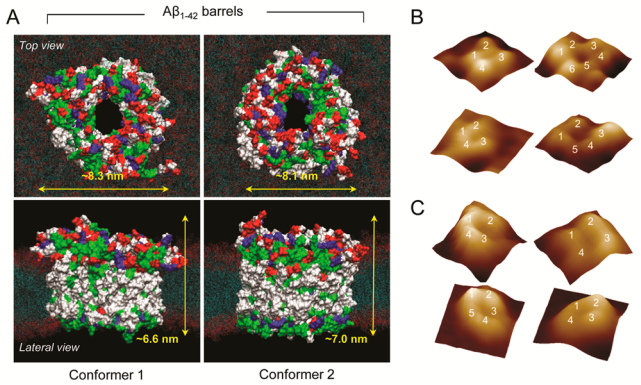

Figure 3. Top and lateral views of simulated (A) $A\beta_{1-42}$ channel structures embedded in the DOPS/POPE lipid bilayer for the conformer 1 and 2 18-mer barrels. The N-terminus side is represented in the upper leaflet and the turn region is represented in the lower leaflet. In the surface representation of the barrel, hydrophobic residues are shown in white, polar and Gly residues are shown in green, positively charged residues are shown in blue, and negatively charged residues are shown in red. For DOPS/POPE lipids, red dots denote the head groups and cyan dots represent the lipid tails. Representative 3D AFM images of pore structures of $A\beta_{1-42}$ in BTLE (B) and in DOPS/POPE (C) membranes. The size of the AFM images is 20 nm × 20 nm and z scale is 1 nm.

number of $A\beta$ monomers involved in the pore, suggesting that large sizes of pore might be possible with a large number of $A\beta$ subunits. However, the pore height across the membrane is almost the same among the different computed conformers, since each conformer contains a distinct turn region. The longer heights of the $A\beta_{1-42}$ barrels compared to the bilayer thickness of ~5 nm suggest that both sides of the full-length $A\beta$ pores protrude from the membrane surface (Figure 3A).

The MD models of the $A\beta_{1-42}$ pores show that the N-terminus of $A\beta_{1-42}$ extends approximately 1−1.5 nm outside of the plane of the DOPS/POPE bilayer, while the turn region at the other bilayer leaflet only protrudes less than 0.5 nm (lateral view in Figure 3A). The calculated extensions of the N-terminus of $A\beta_{1-42}$ protruding out of the membrane in $A\beta_{1-42}$ oligomers agree well with the measured pore heights by AFM (Figures 2 and 3).

Among these oligomer structures imaged by AFM, well-defined $A\beta_{1-42}$ pore structures were observed in both BLTE and DOPS/POPE membranes (Figures 2 and 3). The quality of AFM images can often vary among different samples due to tip degradation, but high resolution imaging, when achieved, still revealed that pore structures are usually composed of 4 to 5 subunits of $A\beta_{1-42}$ oligomers and that the outer diameters of pore structures are comparable to each other with the average diameters of 11.4 ± 1.5 nm (n = 11) in BTLE membranes and 13.9 ± 2.5 nm (n = 12) in DOPS/POPE membranes, and these dimensions are comparable to the previous results found in other lipid membranes[4,9,10,22] (Figure 3B and C).

Ion Conducting Activity of $A\beta_{1-42}$ in BTLE and DOPS/POPE Membranes. We examined the ion conducting activity of $A\beta_{1-42}$ in BTLE and model DOPS/POPE (1:1, wt/wt) lipid membranes, using a BLM electrical recording setup.[9,10,47] Upon addition of $A\beta_{1-42}$ into the recording electrolyte solution, we observed a heterogeneous population of ion current fluctuations by recording current vs time trances under a constant applied potential of 100 mV (Figure 4), consistent with the

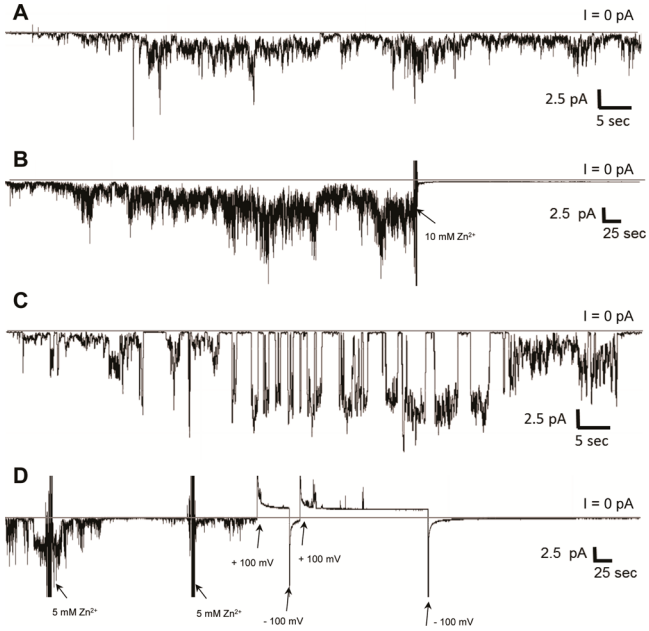

Figure 4. Representative electrical recordings of $A\beta_{1-42}$ in BTLE and DOPS/POPE (1:1, wt/wt) membranes. Current vs time trace of (A) $A\beta_{1-42}$ in a BTLE membrane and (B) inhibition of $A\beta_{1-42}$ conductance by addition of Zn^{2+} (10 mM final $ZnCl_2$ concentration, *cis* chamber). Current vs time trace of (C) $A\beta_{1-42}$ in a DOPS/POPE membrane (D) Inhibition of $A\beta_{1-42}$ conductance by addition of Zn^{2+} in the DOPS/POPE membrane (10 mM final $ZnCl_2$ concentration, *cis* chamber). In all experiments, we used a final concentration of 10 μM $A\beta_{1-42}$ in both chambers of the bilayer setup. Bilayers were formed by the painting method,[57] and a bias potential of ±100 mV was applied. Membrane capacitance was monitored to verify membrane stability. The recording electrolyte consisted of 150 mM KCl, 1 mM $MgCl_2$, and 10 mM HEPES (pH 7.0).

formation of $A\beta_{1-42}$ oligomeric pores of varying size.[48] These transient ion conducting events can be categorized into three types; bursts, steps and spikes.[24] We observed mostly burstlike activities in the current vs time traces of $A\beta_{1-42}$ in the BTLE membrane (Figure 4A and B). Notably, the observed frequency of burstlike events was lower in DOPS/POPE membranes compared to the frequency of bursts in BTLE membranes, while the frequency of well-defined, stepwise current events typically characteristic of ion channels was more pronounced in DOPS/POPE membranes (Figure 4C). Based on these observations of the ion conducting activity of $A\beta_{1-42}$ in the two different types of lipid membranes, we hypothesized that the ion conducting properties of $A\beta$ oligomers are dependent on the composition of lipid head groups that could influence the observed populations of ionic bursts, steps or spikes across

DOI: 10.1021/acschemneuro.7b00006
ACS Chem. Neurosci. 2017, 8, 1348−1357

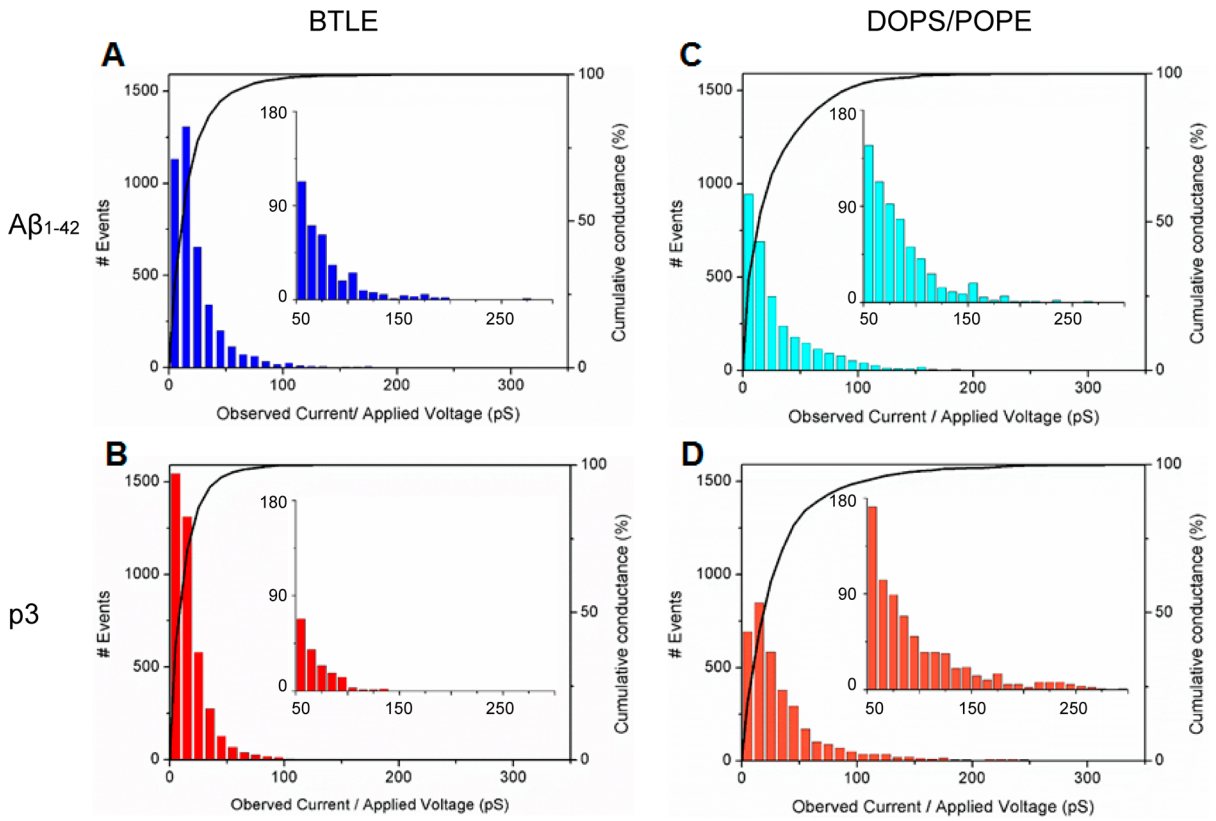

Figure 5. Histograms of frequency vs conductance of ion current fluctuations of Aβ_{1-42} in (A) BTLE membranes or (B) DOPS/POPE membranes and p3 in (C) BTLE membranes or (D) DOPS/POPE membranes. Insets are expanded representation of the histograms from 50 pS to 350 pS (observed current/applied voltage).

membranes. To support this hypothesis, we examined the ion conducting properties of p3 (Aβ_{17-42}), which is a truncated version of Aβ_{1-42} losing many charged amino acid residues that are putatively responsible for interactions with lipid head groups. Similar to the observations with full length Aβ_{1-42} peptides, heterogeneous, burstlike features were dominantly present when p3 was incubated with BTLE membranes, while mostly steplike current events were found when p3 was incubated with DOPS/POPE membranes (see Supporting Information Figure S1A and C). These results support that the electrophysiological characteristics of Aβ oligomers in lipid membranes could be more dependent on lipid compositions rather than peptide sequence. In order to confirm the observed ion conductance across membranes in the BLM experiments was due to the presence of Aβ_{1-42} oligomers, we added Zn^{2+} ions to the recording electrolyte; Zn^{2+} is known to inhibit the ion conducting properties of Aβ in membranes.[49] Upon addition of Zn^{2+} ions into the *cis* chamber of the bilayer setup, the macroscopic conductance of Aβ_{1-42} oligomers decreased gradually and disappeared completely within 5 min in both BTLE and DOPS/POPE membranes (Figure 4B and D). The conductance of p3 peptides was also blocked by Zn^{2+} ions in both BTLE and DOPS/POPE membranes (see Figure S1B and D). We also qualitatively observed that the p3 pore activity appeared faster than for Aβ_{1-42} in most of the experiments using BTLE or DOPS/POPE membranes, perhaps suggesting faster kinetics of insertion and pore formation for p3 in membranes although more experiments would be needed to validate the observation.

We further examined the differences in amplitudes of ion influx through Aβ_{1-42} and p3 pores in BTLE and DOPS/POPE membranes. The amplitudes of ion influx were calculated by dividing each observed current from step and burst events by the applied voltage (Figure 5). Observed amplitude of ion flux values through Aβ_{1-42} ranged between 5 and 200 pS in BTLE membrane and 5−300 pS in DOPS/POPE membrane (Figure 5A and C). In the case of p3, these values varied from 5−140 pS in BTLE membrane and 5−320 pS in DOPS/POPE membranes (Figure 5B and D). The distribution of peaks in both membranes appeared mostly between 10−30 pS. However, both Aβ_{1-42} and p3 oligomers in DOPS/POPE membranes exhibited a higher fraction of current events with conductance above 150 pS (Figure 5C and D inset) compared to their conductance properties in BTLE membranes. In addition, we analyzed the macroscopic ionic flux across the membranes through Aβ_{1-42} and p3 pores by integrating the current traces (i.e., providing an estimate for the total transported charge, Q (C)) over a time period of 5 min (n = 5) for both BTLE and DOPS/POPE membranes (Figure 6). The total transported charge of Aβ_{1-42} and p3 peptides in BTLE and DOPS/POPE membranes is significantly different at the 5% level (p = 0.028) as concluded from a two way ANOVA test. Conversely, the difference in the Q transported by Aβ_{1-42} and p3 pores was found to be statistically insignificant (p = 0.883 and p = 0.614, respectively). We observed an ∼3-fold increase in the average macroscopic ion flux for Aβ_{1-42} in DOPS/POPE membranes compared to the flux through Aβ_{1-42} pores across BTLE membranes and an ∼10-fold increase was observed in the average total transported charge through p3 pores in DOPS/POPE membranes compared to BTLE membranes over the same window of time. The average values for the total transported charges over a 5 min time window

DOI: 10.1021/acschemneuro.7b00006
ACS Chem. Neurosci. 2017, 8, 1348−1357

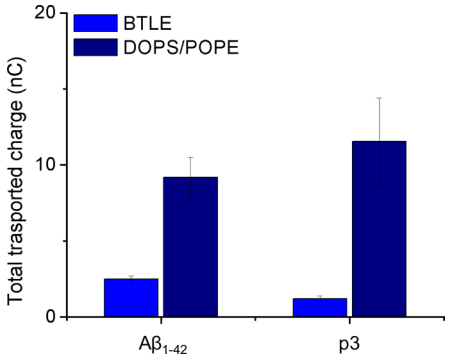

Figure 6. Quantification of ion influx through $A\beta_{1-42}$ and p3 using the total transported charge, Q (nC), in BTLE and DOPS/POPE membranes (n = 5) over a 5 min period of time. Current vs time traces of 11 μM $A\beta_{1-42}$ and 11 μM p3 pore activities were integrated to quantify Q through $A\beta_{1-42}$ and p3 pores (5 min time window, +100 mV). The total transported charge of $A\beta_{1-42}$ and p3 peptides in BTLE and DOPS/POPE membranes is significantly different (p = 0.028) from two way ANOVA test. The data reveal ~3-fold increase in Q for $A\beta_{1-42}$ in DOPS/POPE membranes compared to Q in BTLE membranes, and ~10-fold increase was observed in Q for p3 in DOPS/POPE membranes compared to the Q in BTLE membranes. The electrolyte solution consisted of 150 mM KCl, 1 mM $MgCl_2$, and 10 mM HEPES at pH 7.0. Data represent mean ± standard errors of the mean.

were 2.49 ± 0.20 nC for $A\beta_{1-42}$ and 1.20 ± 0.18 nC for p3 in BTLE membranes, whereas these values were 9.20 ± 1.31 nC for $A\beta_{1-42}$ and 11.55 ± 2.87 nC for p3 in DOPS/POPE membranes (Figure 6).

The interaction of $A\beta_{1-42}$ with BTLE and DOPS/POPE membranes differs considerably in BLM electrical recording (Figure 4). Current vs time traces of $A\beta_{1-42}$ in BTLE membranes show mostly burstlike activities. These results suggest that pores with varying dimensions and subunit composition are active in the membranes. This observation is consistent with the multilevel current events observed for various amyloid pores.[4,10] Previously, we have reported that conductance of $A\beta_{1-42}$ oligomers pores ranged between 30–360 pS in DOPS/POPE (1:1) lipid membranes, with 90% of these current events exhibiting a conductance value of ~33 pS.[24] Even higher conductance (on the order of 1 nS) have been reported for $A\beta_{1-42}$ oligomers in membranes composed of POPE and PS lipid mixtures.[14,50] Current vs time traces of $A\beta_{1-42}$ display burstlike events as well as stepwise current events in DOPS/POPE membranes (Figure 4C). The conductance of $A\beta_{1-42}$ in both of these types of membranes was seen slightly smaller than the previously reported values.

Although it is impractical to study the contribution of each individual lipid components in the BTLE membrane on $A\beta_{1-42}$ pore activity, one potential difference between BTLE and model lipid membranes used for the characterization of Aβ oligomeric pores is the dominance of negatively charged phosphatidylserine (PS) group. PS lipids are one of the major known constituents of BTLE (10.6%, wt/wt) but still less than DOPS/POPE (1:1, wt/wt) lipids. AD brains have higher fraction of PS lipids compared to the brains of cognitively normal, suggesting a possible role of negatively charged lipids in AD pathology.[51−53] We observed a higher frequency of channel-like transmembrane current events from $A\beta_{1-42}$ oligomers in DOPS/POPE membranes compared to the ion transport activity of this peptide in BTLE membranes (Figure 4).

In addition, the frequency of burstlike ion conducting events from Aβ pores in BTLE membranes was lower than in DOPS/POPE membranes. These observations could arise from a variety of reasons. First, different interactions of $A\beta_{1-42}$ peptides with the lipid head groups could affect the current events. Second, there are potential differences in phase transition temperature (T_m) of the lipids within the membranes. For example, the T_m of POPE lipid is 24 °C while the T_m of BTLE is not known. Additionally, low stability of the pore structures in BTLE membranes could shorten the lifetime of the activities and cause an overlap between current events. To shed some light on a possible cause for the different conductance properties of $A\beta_{1-42}$ oligomers in different membranes, we examined the transmembrane ion transport properties of p3 peptides in both BTLE and DOPS/POPE lipid membranes. Since the charged residues of $A\beta_{1-42}$ that can interact with the head groups of the lipids are mostly located in the N-terminal region of $A\beta_{1-42}$, p3, as a truncated version of $A\beta_{1-42}$, can reveal if the interaction of the N-terminal region of full length $A\beta_{1-42}$ with the lipid headgroups can affect the ion conducting characteristics of $A\beta_{1-42}$ in membranes. We observed a trend of more burstlike current events with p3 peptides in BTLE membranes, whereas we observed more steplike current events of this peptide in DOPS/POPE membranes (see Supporting Information Figure S1). We observed that current events from p3 peptides in DOPS/POPE appeared less stepwise than the current events observed for $A\beta_{1-42}$. The effect of T_m of POPE lipids on current events was also inspected by replacing the POPE in DOPS/POPE membranes with 1,2-dioleoyl-*sn*-glycero-3-phosphoethanolamine (DOPE) (to form DOPS/DOPE membranes), which has a T_m of −16 °C. The ion conducting properties of $A\beta_{1-42}$ in DOPS/DOPE (1:1, wt/wt) membranes show comparable steplike channel events to the ion conducting properties of $A\beta_{1-42}$ in DOPS/POPE (1:1, wt/wt) membranes, suggesting that T_m of the lipid does not influence the formation of steplike current fluctuations of $A\beta_{1-42}$ in membranes (see Supporting Information Figure S2).

We hypothesize that the presence of Aβ oligomeric pores with higher conductance values in DOPS/POPE membranes compared to BTLE membranes may imply that Aβ oligomers could have increased detrimental effects in patients with AD compared to healthy patients, as DOPS/POPE membranes contain higher percentages of PS lipids than BTLE membranes, potentially mimicking an important difference between the lipid compositions in diseased vs healthy brains. The BTLE membranes used here contain only 10.6% PS (see Supporting Information Table1), potentially representing a model for healthy brains. Thus, $A\beta_{1-42}$ oligomers in BTLE membranes displayed more heterogeneous current events, lower average amplitudes of conductance for individual ion fluctuations, and reduced macroscopic ion flux compared to the conductance properties of this peptide in DOPS/POPE membranes. Previous studies showed that $A\beta_{25-35}$ (a neurotoxic fragment of $A\beta_{1-42}$) could form ion conducting pores in membranes derived from a total brain lipid extract. However, in a lipid membrane extracted from soybeans,[30] cholesterol in the membrane was shown to inhibit formation of ion conducting $A\beta_{25-35}$ pores,[30] and this finding with cholesterol was replicated with the inhibition of the formation of ion conducting $A\beta_{1-42}$ oligomers in cellular membranes.[12,54] Anionic lipids have

DOI: 10.1021/acschemneuro.7b00006
ACS Chem. Neurosci. 2017, 8, 1348−1357

previously been suggested to promote the formation of ion conducting Aβ oligomeric pores.[29,30] The membrane disruption was shown to follow a two step mechanism with the initial formation of pores and nonspecific membrane fragmentation.[55,56] The present findings are consistent with these previous results, and suggest that lipids derived from brains provide a relatively unfavorable environment for the formation of Aβ pores, but still permit their formation under some conditions. This is unsurprising given the late development and slow progression of sporadic AD cases. However, we have shown that Aβ pore formation is possible in BTLE membranes providing a viable mechanism of early stage AD pathology. As lipid composition shifts to more anionic head groups during disease progression, this effect would only be intensified as demonstrated by the current events of Aβ oligomers in DOPS/POPE membranes. Although further investigation of Aβ oligomer structures in various lipid compositions using more detailed structural techniques, including NMR or EPR, would be helpful to characterize the effects of lipid headgroups on Aβ aggregation, the results reported here suggest that regions containing high fractions of anionic lipids (especially with PS head groups) could provide a favorable environment promoting the formation and insertion of Aβ pores in membranes.

CONCLUSIONS

We have investigated the structures, ion conducting properties, and self-assembly kinetics of the full-length $A\beta_{1-42}$ peptide in lipid bilayers composed of brain total lipid extract (BTLE) and a model lipid mixture comprised of DOPS/POPE (1:1 wt/wt). $A\beta_{1-42}$ peptides aggregate faster when BTLE or DOPS/POPE liposomes were present in solution. $A\beta_{1-42}$ oligomers insert into both type of the membranes, forming ion-conducting pore structures that can be blocked by Zn^{2+} ions. However, the ion conducting properties of $A\beta_{1-42}$ oligomers, as well as the distribution of subpopulations of membrane-associated oligomers differ as a function of lipid composition. The presence of heterogeneous bursts of ion fluctuations was observed for $A\beta_{1-42}$ in BTLE membranes, which may reflect a heterogeneous population of sizes of porelike structures found when this peptide was reconstituted in BTLE membranes. Conversely, $A\beta_{1-42}$ in DOPS/POPE membranes reveal more stepwise current events, which could reflect the presence of a different heterogeneous population of oligomeric pores found in DOPS/POPE membranes by AFM. Additionally, to examine the effect of interactions of the N-terminal residues of $A\beta_{1-42}$ with the membrane surface on ion conducting properties, we observed similar trends of burstlike current events in BTLE membranes and more stepwise current events in DOPS/POPE membranes for p3 peptides (which lacked the charged N-terminal residues present in full length Aβ). While additional molecular details for the formation of $A\beta_{1-42}$ in BTLE membranes remain to be established, both full-length Aβ peptides and its nonamyloidogenic p3 fragment form pores in BTLE membranes, suggesting that both Aβ peptides have the capability to alter neuronal cell homeostasis and play toxic roles in the brain. Hence, these oligomeric Aβ structures could serve as specific targets for the development of therapeutic strategies for the treatment AD.

METHODS

Peptide Preparation. All $A\beta_{1-42}$ and $A\beta_{17-42}$ had >90% purity as provided by the manufacturer (Anaspec, Fremont, CA and rPeptide, Bogart, GA). The initial powders were first dissolved in 1% ammonium hydroxide until the peptides were completely dissolved. They were subsequently sonicated for approximately 2 min. The desired amount of peptide was then aliquoted and lyophilized using a lyophilizer (FreeZone 2.5 Plus, Labconco, Kansas City, KS). The aliquots were stored at −80 °C for a maximum of 3 months until they were used. For each experiment, aliquoted peptides were taken from −80 °C and dissolved first in 10 mM NaOH and diluted with 10 mM HEPES (1 mM $MgCl_2$, 150 mM KCl, pH = 7.4) buffer solutions to make final concentration of 100 μM. Percentage of NaOH in the solution never exceeds more than 10% and the pH was changed less than 1%. The peptide concentration was measured using the 280 nm UV absorbance (extinction coefficient: ε = 1490 M^{-1} cm^{-1}).

Thioflavin T Assay. ThT assay was conducted as previously described.[23] Briefly, 10 μM ThT solution was prepared using 10 mM HEPES (1 mM $MgCl_2$, 150 mM KCl, pH = 7.4) buffer in 96-well white-walled plates (Nunc). Using 10 mM NaOH, lyophilized peptide was dissolved to prevent aggregation. The peptide solution was then diluted with the HEPES buffer to its final peptide concentration of 10 μM in the plate well. For monitoring the effect of liposomes in Aβ self-assembly, 0.2 mg/mL liposomes of BTLE and DOS/POPE (1:1, wt/wt) were prepared by extrusion method using a 100 nm membrane filter and the either BTLE or DOPS/POPE liposomes were added instead of the buffer in the well. The NaOH content was maintained at <10% of the total volume. ThT fluorescence (450 nm excitation, 490 nm emission) was monitored every 5 min at 25 °C for the indicated times using a SPECTRAmax Gemini EM fluorescent plate reader (Molecular Devices, Sunnyvale, CA).

Proteoliposome Preparation for AFM Imaging. For preparation of supported lipid bilayers, 40 μL of brain total lipid extract (BTLE) or DOPS/POPE (1:1, wt/wt) lipids (Avanti Polar Lipids, Alabaster, AL) in chloroform was first added to a clean 2.5 mL vial. Chloroform was evaporated using a vacuum pump or a rotary evaporator to produce a lipid film. The dried lipid film was hydrated for an hour with 10 mM HEPES (1 mM $MgCl_2$, 150 mM KCl, pH = 7.4) buffer to a final concentration of 0.1−0.5 mg/mL at 25 °C under occasional vortexing. Finally, the liposome solutions were sonicated for 5 min and stored in a 4 °C until used.

To achieve high insertions of $A\beta_{1-42}$ or p3 peptides in BTLE or DOPS/POPE membranes, lipids were hydrated with peptide-containing solutions at ∼1:20 peptide/lipid mass ratios (Figure 2). Otherwise, lipids were hydrated in HEPES buffer containing 0.5−1 mg/mL peptide concentrations. They were vortexed vigorously for 30 sec at 5 min intervals and subsequently sonicated for 5 min in an ice bath. The peptide to lipid mass ratios of 1:20 for $A\beta_{1-42}$ and 1:7 for p3 were used. For AFM imaging, ∼10 μL of the sample solution was deposited on freshly cleaved mica and incubated for ∼1−3 min to form supported lipid bilayers by vesicle rupture on the mica surface. After incubation, samples were rinsed with the buffer to remove unruptured liposomes in the solution. Topographic images $A\beta_{1-42}$ and p3 in BTLE or DOPS/POPE membranes were acquired using a Multimode AFM equipped with a Nanoscope V controller (Bruker, Santa Barbara, CA). Silicon nitride cantilevers with a nominal spring constant of 0.08 N/m (TR400PSA, Asylum Research, Goleta, CA) were employed using regular tapping mode as well as peak-force tapping. The Nanoscope software was used for analyzing imaging data.

Formation of Planar Lipid Bilayers for BLM Experiments. We formed planar lipid bilayers by the "painting method" over a 250 μm aperture in a Delrin cup (1 mL volume, Warner Instruments, Hamden, CT).[57] This aperture was first pretreated with ∼2 μL of 20 mg/mL BTLE, DOPS/POPE (1:1, wt/wt), or DOPS/DOPE (1:1, wt/wt) lipid in hexane. Following pretreatment, a solution of 10 mM HEPES, 150 mM KCl, 1 mM $MgCl_2$, pH 7.0 (recording solution) was added to both chambers. Subsequently, a 20 mg/mL solution of BTLE lipid, DOPS/POPE (1:1, wt/wt), or DOPS/DOPE (1:1, wt/wt) in *n*-decane was added over the aperture using a fine tip paintbrush until a bilayer was formed. During this process, the capacitance of the bilayer was monitored to check the thinning of the lipid and decane droplet. If the droplet did not thin spontaneously, we applied air-bubbles using a micron pipet under the pore to facilitate the thinning of the lipid-decane droplet. When the lipid bilayer was stable for more than 30 min

DOI: 10.1021/acschemneuro.7b00006
ACS Chem. Neurosci. 2017, 8, 1348−1357

within ±100 mV applied potential and the capacitance of the bilayer was above 130 pF, we added 11−22 μM Aβ_{1-42} or p3 directly into the chamber. The chamber was stirred with a stirring bar by using Stir-2 stir plate (Warner Instruments, Hamden, CT) for 5 min to help Aβ peptides access the lipid bilayer easily.

BLM Measurements of Aβs. We performed channel activity recordings in "voltage clamp mode" using Ag/AgCl electrodes (Warner Instruments, Hamden, CT) immersed in each chamber. Data acquisition and storage were carried out using custom-made LabVIEW software in combination with a BC-535 patch clamp amplifier (set at a gain of 10 mV/pA and a filter cutoff frequency of 3 kHz, Warner Instruments, Hamden, CT). The data were acquired at a sampling frequency of 15 kHz using a data acquisition board (National Instruments, Austin, TX) connected to the amplifier. We conducted filtering using a digital Gaussian low-pass filter (cutoff frequency of 50 Hz) by ClampFit 9.2 software (Axon Instruments; Molecular devices, Sunnyvale, CA). All experiments were conducted for 60−80 min after adding the corresponding peptide solution. For channel blockage experiments, a final concentration of 2 mM $ZnCl_2$ solution was added to one side of the chamber. We analyzed the ion influx through Aβ_{1-42} and p3 peptides by integrating the current (over t = 5 min) in current vs time traces to characterize the heterogeneous conductances of both the peptides. This area represents the total transported charge during the chosen time interval.

total transported charge

$$Q = \int_{t=0}^{t=5\text{min}} I(t)\mathrm{d}t \tag{3}$$

We used this equation to characterize Aβ_{1-42} and p3 porelike structures.

A two way ANOVA test with the membrane types and peptide types as two independent variables and total transported charges as the dependent variable was carried out to account for the contributions of the membranes, peptides, or interaction of both.

Before introducing any Aβ peptides into the BLM cup, we monitored that the electrical current traces did not display leakage currents. The capacitance of the membrane was monitored occasionally to check the stability of the membrane. Aβ peptides were only introduced in the membrane when the capacitance was higher than 130 pF and stable at least for 30 min. We also confirmed the pore activities by changing the polarity from 100 to −100 mV and confirming that the measured ionic currents changed accordingly during the activity recording.

■ ASSOCIATED CONTENT

Supporting Information

The Supporting Information is available free of charge on the ACS Publications website at DOI: 10.1021/acschemneuro.7b00006.

Representative electrical recordings of p3 peptides in BTLE and DOPS/POPE (1:1, wt/wt) membranes, Aβ_{1-42} in a DOPS/DOPE (1:1, wt/wt) membrane, and composition of brain total lipid extract (PDF)

■ AUTHOR INFORMATION

ORCID

Joon Lee: 0000-0003-3887-8540

Alan L. Gillman: 0000-0002-1312-047X

Jerry Yang: 0000-0002-8423-7376

Author Contributions

J.L., Y.H.K., and F.T.A. contributed equally to this work. J.L., Y.H.K., and R.L. designed the study. J.L. and F.T.A. performed AFM imaging. J.L. and Y.H.K. performed electrical recording. H.J. performed MD simulation. J.L., Y.H.K., F.T.A., and H.J. wrote the manuscript. A.G., B.K., R.N., J.Y., and R.L. revised the manuscript. All authors reviewed the manuscript.

Funding

This project was supported by the National Institute on Aging of National Institutes of Health (Grant AG028709). Y.H.K and J.Y. acknowledge support from the Air Force Office of Scientific Research (FA9550-12-1-0435) and from the National Institute on Aging of the National Institutes of Health under Award Number R01AG053577. The fund from Frontier Innovation Scholars Program in UCSD supported to J.L. This project has been funded in whole or in part with Federal funds from the Frederick National Laboratory for Cancer Research, National Institutes of Health, under contract HHSN261200800001E. This research was supported [in part] by the Intramural Research Program of NIH, Frederick National Lab, Center for Cancer Research. The content of this publication does not necessarily reflect the views or policies of the Department of Health and Human Services, nor does mention of trade names, commercial products or organizations imply endorsement by the US Government.

Notes

The authors declare no competing financial interest.

■ ACKNOWLEDGMENTS

All simulations had been performed using the high-performance computational facilities of the Biowulf PC/Linux cluster at the National Institutes of Health, Bethesda, MD (http://biowulf.nih.gov). We would like to acknowledge Abhijith G Karkisaval for help with the statistical analysis.

■ REFERENCES

(1) Masters, C. L., Simms, G., Weinman, N. A., Multhaup, G., McDonald, B. L., and Beyreuther, K. (1985) Amyloid plaque core protein in Alzheimer disease and Down syndrome. *Proc. Natl. Acad. Sci. U. S. A. 82*, 4245−4249.

(2) Thinakaran, G., and Koo, E. H. (2008) Amyloid precursor protein trafficking, processing, and function. *J. Biol. Chem. 283*, 29615−29619.

(3) Miller, Y., Ma, B., and Nussinov, R. (2009) Polymorphism of Alzheimer's Aβ17−42 (p3) Oligomers: The Importance of the Turn Location and Its Conformation. *Biophys. J. 97*, 1168−1177.

(4) Jang, H., Arce, F. T., Ramachandran, S., Capone, R., Azimova, R., Kagan, B. L., Nussinov, R., and Lal, R. (2010) Truncated β-amyloid peptide channels provide an alternative mechanism for Alzheimer's disease and Down syndrome. *Proc. Natl. Acad. Sci. U. S. A. 107*, 6538−6543.

(5) Jang, H., Teran Arce, F., Ramachandran, S., Capone, R., Lal, R., and Nussinov, R. (2010) Structural convergence among diverse, toxic beta-sheet ion channels. *J. Phys. Chem. B 114*, 9445−9451.

(6) Hardy, J., and Selkoe, D. J. (2002) The amyloid hypothesis of Alzheimer's disease: progress and problems on the road to therapeutics. *Science 297*, 353−356.

(7) Lasagna-Reeves, C. A., Glabe, C. G., and Kayed, R. (2011) Amyloid-β annular protofibrils evade fibrillar fate in Alzheimer disease brain. *J. Biol. Chem. 286*, 22122−30.

(8) Bhatia, R., Lin, H., and Lal, R. (2000) Fresh and globular amyloid beta protein (1−42) induces rapid cellular degeneration: evidence for AbetaP channel-mediated cellular toxicity. *FASEB J. 14*, 1233−43.

(9) Lin, H. A. I., Bhatia, R., and Lal, R. (2001) Amyloid β protein forms ion channels: Implications for Alzheimer's disease pathophysiology. *FASEB J. 15*, 2433−2444.

(10) Quist, A., Doudevski, I., Lin, H., Azimova, R., Ng, D., Frangione, B., Kagan, B., Ghiso, J., and Lal, R. (2005) Amyloid ion channels: a common structural link for protein-misfolding disease. *Proc. Natl. Acad. Sci. U. S. A. 102*, 10427−32.

DOI: 10.1021/acschemneuro.7b00006
ACS Chem. Neurosci. 2017, 8, 1348−1357

(11) Bezprozvanny, I., and Mattson, M. P. (2008) Neuronal calcium mishandling and the pathogenesis of Alzheimer's disease. *Trends Neurosci. 31*, 454−63.
(12) Kawahara, M., and Kuroda, Y. (2001) Intracellular Calcium Changes in Neuronal Cells Induced by Alzheimer's ß-Amyloid Protein Are Blocked by Estradiol and Cholesterol. *Cell. Mol. Neurobiol. 21*, 1−13.
(13) Kagan, B. L., Hirakura, Y., Azimov, R., Azimova, R., and Lin, M.-C. (2002) The channel hypothesis of Alzheimer's disease: current status. *Peptides 23*, 1311−1315.
(14) Arispe, N., Pollard, H. B., and Rojas, E. (1993) Giant multilevel cation channels formed by Alzheimer disease amyloid beta-protein [A beta P-(1−40)] in bilayer membranes. *Proc. Natl. Acad. Sci. U. S. A. 90*, 10573−7.
(15) Demuro, A., Smith, M., and Parker, I. (2011) Single-channel Ca(2+) imaging implicates Aβ1−42 amyloid pores in Alzheimer's disease pathology. *J. Cell Biol. 195*, 515−24.
(16) Wei, W. (2002) Abeta 17−42 in Alzheimer's disease activates JNK and caspase-8 leading to neuronal apoptosis. *Brain 125*, 2036−2043.
(17) Di Scala, C., Troadec, J.-D., Lelièvre, C., Garmy, N., Fantini, J., and Chahinian, H. (2014) Mechanism of cholesterol-assisted oligomeric channel formation by a short Alzheimer β-amyloid peptide. *J. Neurochem. 128*, 186−95.
(18) Arce, F. T., Jang, H., Ramachandran, S., Landon, P. B., Nussinov, R., and Lal, R. (2011) Polymorphism of amyloid β peptide in different environments: implications for membrane insertion and pore formation. *Soft Matter 7*, 5267.
(19) Czajkowsky, D. M., Sheng, S., and Shao, Z. (1998) Staphylococcal α-hemolysin can form hexamers in phospholipid bilayers1. *J. Mol. Biol. 276*, 325−330.
(20) Lashuel, H. A., Hartley, D., Petre, B. M., Walz, T., and Lansbury, P. T., Jr (2002) Neurodegenerative disease: Amyloid pores from pathogenic mutations. *Nature 418*, 291.
(21) Jang, H., Arce, F. T., Ramachandran, S., Capone, R., Lal, R., and Nussinov, R. (2010) β-Barrel Topology of Alzheimer's β-Amyloid Ion Channels. *J. Mol. Biol. 404*, 917−934.
(22) Connelly, L., Jang, H., Teran Arce, F., Capone, R., Kotler, S. A., Ramachandran, S., Kagan, B. L., Nussinov, R., and Lal, R. (2012) Atomic Force Microscopy and MD Simulations Reveal Pore-Like Structures of All-d-Enantiomer of Alzheimer's β-Amyloid Peptide: Relevance to the Ion Channel Mechanism of AD Pathology. *J. Phys. Chem. B 116*, 1728−1735.
(23) Lee, J., Gillman, A. L., Jang, H., Ramachandran, S., Kagan, B. L., Nussinov, R., and Teran Arce, F. (2014) Role of the Fast Kinetics of Pyroglutamate-Modified Amyloid-β Oligomers in Membrane Binding and Membrane Permeability. *Biochemistry 53*, 4704−4714.
(24) Gillman, A. L., Jang, H., Lee, J., Ramachandran, S., Kagan, B. L., Nussinov, R., and Teran Arce, F. (2014) Activity and Architecture of Pyroglutamate-Modified Amyloid-β (AβpE3−42) Pores. *J. Phys. Chem. B 118*, 7335−7344.
(25) Arispe, N., Pollard, H. B., and Rojas, E. (1996) Zn2+ interaction with Alzheimer amyloid beta protein calcium channels. *Proc. Natl. Acad. Sci. U. S. A. 93*, 1710−1715.
(26) Hirakura, Y., Lin, M.-C., and Kagan, B. L. (1999) Alzheimer amyloid aβ1−42 channels: Effects of solvent, pH, and congo red. *J. Neurosci. Res. 57*, 458−466.
(27) Di Paolo, G., and Kim, T.-W. W. (2011) Linking lipids to Alzheimer's disease: cholesterol and beyond. *Nat. Rev. Neurosci. 12*, 284−96.
(28) Mendis, L. H. S., Grey, A. C., Faull, R. L. M., and Curtis, M. A. (2016) Hippocampal lipid differences in Alzheimer's disease: a human brain study using matrix-assisted laser desorption/ionization-imaging mass spectrometry. *Brain Behav. 6*, e00517.
(29) Alarcón, J. M., Brito, J. A., Hermosilla, T., Atwater, I., Mears, D., and Rojas, E. (2006) Ion channel formation by Alzheimer's disease amyloid β-peptide (Aβ40) in unilamellar liposomes is determined by anionic phospholipids. *Peptides 27*, 95−104.
(30) Lin, M. A., and Kagan, B. L. (2002) Electrophysiologic properties of channels induced by Aβ25−35 in planar lipid bilayers. *Peptides 23*, 1215−1228.
(31) Meleleo, D., Galliani, A., and Notarachille, G. (2013) AβP1−42 incorporation and channel formation in planar lipid membranes: the role of cholesterol and its oxidation products. *J. Bioenerg. Biomembr. 45*, 369−381.
(32) Sani, M.-A., Gehman, J. D., and Separovic, F. (2011) Lipid matrix plays a role in Abeta fibril kinetics and morphology. *FEBS Lett. 585*, 749−54.
(33) LeVine, H., III (1999) Quantification of β-sheet amyloid fibril structures with thioflavin T. In *Amyloid, Prions, and Other Protein Aggregates* (Abelson, J., Simon, M., and Wetzel, R., Eds.), pp 274−284, Academic Press, New York.
(34) Biancalana, M., and Koide, S. (2010) Molecular mechanism of Thioflavin-T binding to amyloid fibrils. *Biochim. Biophys. Acta, Proteins Proteomics 1804*, 1405−12.
(35) Lomakin, A., Chung, D. S., Benedek, G. B., Kirschner, D. A., and Teplow, D. B. (1996) On the nucleation and growth of amyloid beta-protein fibrils: detection of nuclei and quantitation of rate constants. *Proc. Natl. Acad. Sci. U. S. A. 93*, 1125−1129.
(36) Nielsen, L., Khurana, R., Coats, A., Frokjaer, S., Brange, J., Vyas, S., Uversky, V. N., and Fink, A. L. (2001) Effect of Environmental Factors on the Kinetics of Insulin Fibril Formation: Elucidation of the Molecular Mechanism. *Biochemistry 40*, 6036−6046.
(37) Shimanouchi, T., Onishi, R., Kitaura, N., Umakoshi, H., and Kuboi, R. (2011) Copper-mediated growth of amyloid β fibrils in the presence of oxidized and negatively charged liposomes. *J. Biosci. Bioeng. 112*, 611−615.
(38) Conway, K. A., Lee, S.-J. J., Rochet, J. C., Ding, T. T., Williamson, R. E., and Lansbury, P. T. (2000) Acceleration of oligomerization, not fibrillization, is a shared property of both α-synuclein mutations linked to early-onset Parkinson's disease: Implications for pathogenesis and therapy. *Proc. Natl. Acad. Sci. U. S. A. 97*, 571−576.
(39) Parbhu, A., Lin, H., Thimm, J., and Lal, R. (2002) Imaging real-time aggregation of amyloid beta protein (1−42) by atomic force microscopy. *Peptides 23*, 1265−1270.
(40) Vivekanandan, S., Brender, J. R., Lee, S. Y., and Ramamoorthy, A. (2011) A partially folded structure of amyloid-beta(1−40) in an aqueous environment. *Biochem. Biophys. Res. Commun. 411*, 312−6.
(41) Suzuki, Y., Brender, J. R., Soper, M. T., Krishnamoorthy, J., Zhou, Y., Ruotolo, B. T., Kotov, N. A., Ramamoorthy, A., and Marsh, E. N. G. (2013) Resolution of Oligomeric Species during the Aggregation of Aβ1−40 Using 19F NMR. *Biochemistry 52*, 1903−1912.
(42) Bernstein, S. L., Dupuis, N. F., Lazo, N. D., Wyttenbach, T., Condron, M. M., Bitan, G., Teplow, D. B., Shea, J.-E. E., Ruotolo, B. T., Robinson, C. V., and Bowers, M. T. (2009) Amyloid-beta protein oligomerization and the importance of tetramers and dodecamers in the aetiology of Alzheimer's disease. *Nat. Chem. 1*, 326−331.
(43) Eisenberg, D., and Jucker, M. (2012) The Amyloid State of Proteins in Human Diseases. *Cell 148*, 1188−1203.
(44) Connelly, L., Jang, H., Teran Arce, F., Ramachandran, S., Kagan, B. L., Nussinov, R., and Lal, R. (2012) Effects of Point Substitutions on the Structure of Toxic Alzheimer's β-Amyloid Channels: Atomic Force Microscopy and Molecular Dynamics Simulations. *Biochemistry 51*, 3031−3038.
(45) Jang, H., Teran Arce, F., Ramachandran, S., Kagan, B. L., Lal, R., and Nussinov, R. (2013) Familial Alzheimer's Disease Osaka Mutant (ΔE22) β-Barrels Suggest an Explanation for the Different Aβ1−40/42 Preferred Conformational States Observed by Experiment. *J. Phys. Chem. B 117*, 11518−11529.
(46) Jang, H., Teran Arce, F., Ramachandran, S., Kagan, B. L., Lal, R., and Nussinov, R. (2014) Disordered amyloidogenic peptides may insert into the membrane and assemble into common cyclic structural motifs. *Chem. Soc. Rev. 43*, 6750.
(47) Capone, R., Jang, H., Kotler, S. a., Kagan, B. L., Nussinov, R., and Lal, R. (2012) Probing Structural Features of Alzheimer's

DOI: 10.1021/acschemneuro.7b00006
ACS Chem. Neurosci. 2017, 8, 1348−1357

Amyloid-β Pores in Bilayers Using Site-Specific Amino Acid Substitutions. *Biochemistry 51*, 776−785.
(48) Jang, H., Arce, F. T., Capone, R., Ramachandran, S., Lal, R., and Nussinov, R. (2009) Misfolded Amyloid Ion Channels Present Mobile β-Sheet Subunits in Contrast to Conventional Ion Channels. *Biophys. J. 97*, 3029−3037.
(49) Capone, R., Jang, H., Kotler, S. A., Connelly, L., Teran Arce, F., Ramachandran, S., Kagan, B. L., Nussinov, R., and Lal, R. (2012) All-d-Enantiomer of β-Amyloid Peptide Forms Ion Channels in Lipid Bilayers. *J. Chem. Theory Comput. 8*, 1143−1152.
(50) Arispe, N., Rojas, E., and Pollard, H. B. (1993) Alzheimer disease amyloid β protein forms calcium channels in bilayer membranes: Blockade by tromethamine and aluminum. *Proc. Natl. Acad. Sci. U. S. A. 90*, 567−571.
(51) Wells, K., Farooqui, A., Liss, L., and Horrocks, L. (1995) Neural membrane phospholipids in alzheimer disease. *Neurochem. Res. 20*, 1329−1333.
(52) Lee, G., Pollard, H. B., and Arispe, N. (2002) Annexin 5 and apolipoprotein E2 protect against Alzheimer's amyloid-β-peptide cytotoxicity by competitive inhibition at a common phosphatidylserine interaction site. *Peptides 23*, 1249−1263.
(53) Arispe, N., Diaz, J. C., and Simakova, O. (2007) Aβ ion channels. Prospects for treating Alzheimer's disease with Aβ channel blockers. *Biochim. Biophys. Acta, Biomembr. 1768*, 1952−1965.
(54) ARISPE, N. (2002) Plasma membrane cholesterol controls the cytotoxicity of Alzheimer's disease AbetaP (1−40) and (1−42) peptides. *FASEB J. 16*, 1526−1536.
(55) Sciacca, M., Kotler, S., Brender, J., Chen, J., Lee, D.-k., and Ramamoorthy, A. (2012) Two-Step Mechanism of Membrane Disruption by A β through Membrane Fragmentation and Pore Formation. *Biophys. J. 103*, 702−710.
(56) Kotler, S. A., Walsh, P., Brender, J. R., and Ramamoorthy, A. (2014) Differences between amyloid-β aggregation in solution and on the membrane: insights into elucidation of the mechanistic details of Alzheimer's disease. *Chem. Soc. Rev. 43*, 6692.
(57) Capone, R., Blake, S., Rincon Restrepo, M., Yang, J., and Mayer, M. (2007) Designing Nanosensors Based on Charged Derivatives of Gramicidin A. *J. Am. Chem. Soc. 129*, 9737−9745.

DOI: 10.1021/acschemneuro.7b00006
ACS Chem. Neurosci. 2017, 8, 1348−1357